

Spin wave dispersion relation in $\text{Sr}_2\text{Cu}_3\text{O}_4\text{Cl}_2$ lattice structure

Solange Flatt

Co-supervisor : Noore Elahi Shaik

Supervisor : Pr. H. M. Rønnow

carried out in the *Laboratory for Quantum Magnetism* (LQM)

January 14, 2016

Contents

1	Introduction	2
2	Theory	2
2.1	Definition of the coupling	2
2.2	Calculation of the spin wave dispersion relation for a $2D$ square lattice . .	3
3	Crystal structure	5
3.1	Plane structure	5
3.2	3D Structure	5
4	Reciprocal space	6
5	Coupling between two sites	6
5.1	Description of the algorithm	6
5.2	Results	7
6	Spin wave relation dispersion	11
7	Conclusion	14
8	References	15

1 Introduction

The aim of this project is to compute the spin wave dispersion of the $\text{Sr}_2\text{Cu}_3\text{O}_4\text{Cl}_2$ like lattice. After having introduced the necessary theoretical elements and the crystallographic structure of $\text{Sr}_2\text{Cu}_3\text{O}_4\text{Cl}_2$, we will first calculate the couplings between two sites of the lattice. The second main part is to compute the spin wave dispersion relation, in function of the coupling previously calculated.

2 Theory

A simple microscopic model to describe the electrons in strong correlated systems on a lattice is the Hubbard model. In this model, the Hamiltonian is given by equation 1 :

$$\mathcal{H} = -t \underbrace{\sum_{\langle ij \rangle, \sigma} (c_{i\sigma}^\dagger c_{j\sigma} + h.c.)}_T + U \underbrace{\sum_i n_{i\uparrow} n_{i\downarrow}}_V \quad (1)$$

Where $n_{i\sigma}$ in terms of the operator c is : $n_{i\sigma} = c_{i\sigma}^\dagger c_{i\sigma}$.

The assumption in our case is made that we are in the case of a strong coupling limit (i.e $t \ll U$). The cost in energy to have two electrons on the same site is very large. As a consequence, the Hamiltonian 1 can be developed using the perturbation theory.

The derivation will not be developed here, but after some calculations (refer to [1]) it can be shown that the effective spin Hamiltonian is :

$$\begin{aligned} \hat{\mathcal{H}} = & \sum_{\left\{ \begin{array}{c} \text{---} \\ \text{---} \\ \text{---} \\ \text{---} \\ \text{---} \\ \text{---} \end{array} \right\}} \left(\frac{4t_{12}^2}{U} - \frac{16t_{12}^4}{U^3} \right) \left(\vec{S}_1 \cdot \vec{S}_2 - \frac{1}{4} \right) \\ & + \sum_{\left\{ \begin{array}{c} \text{---} \\ \text{---} \\ \text{---} \\ \text{---} \\ \text{---} \\ \text{---} \end{array} \right\}} \frac{4t_{12}^2 t_{23}^2}{U^3} \left(\vec{S}_1 \cdot \vec{S}_3 - \frac{1}{4} \right) \\ & - \sum_{\left\{ \begin{array}{c} \text{---} \\ \text{---} \\ \text{---} \\ \text{---} \\ \text{---} \\ \text{---} \end{array} \right\}} \frac{4t_{12} t_{23} t_{34} t_{41}}{U^3} \left\{ \sum_{\substack{i,j=1 \\ i \neq j}}^4 \vec{S}_i \cdot \vec{S}_j - 20 \left[\left(\vec{S}_1 \cdot \vec{S}_2 \right) \left(\vec{S}_3 \cdot \vec{S}_4 \right) + \left(\vec{S}_1 \cdot \vec{S}_4 \right) \left(\vec{S}_2 \cdot \vec{S}_3 \right) - \left(\vec{S}_1 \cdot \vec{S}_3 \right) \left(\vec{S}_2 \cdot \vec{S}_4 \right) \right] \right\} \\ & + E^{(4)} \end{aligned} \quad (2)$$

The development of the Hamiltonian is made to the fourth order, i.e we neglect terms of higher order than $\frac{t^4}{U^3}$. This approximation is justified by the fact that $t \ll U$.

2.1 Definition of the coupling

From the formula 2, we can define the coupling $J_{(i,j)}$ between two given sites i and j . The coupling is the sum of three contributions :

- the two site coupling : if the site i and the site j are connected by a possible hopping, the contribution is

$$\left(\frac{4t_{ij}^2}{U} - \frac{16t_{ij}^4}{U^3} \right) \quad (3)$$

- the three site coupling: we have to consider all the sites k such that the sites i and k are connected, as well as the sites k and j . The total contribution is equal to

$$\sum_k \frac{4t_{ik}^2 t_{kj}^2}{U^3} \quad (4)$$

- the four site coupling : all the possible closed loops that go through site i and site j contribute. For this term, two additional distinctions have to be considered :

- Either i and j are neighbour in the loop. In other words, there are the sites k and l such that $ijkl$ is a closed loop. The effective contribution to spin wave comes from Heisenberg like coupling

$$- \frac{4t_{ij}t_{jk}t_{kl}t_{li}}{U^3} \left(1 - 20\vec{S}_k \cdot \vec{S}_l \right) \quad (5)$$

- Or i and j are on the diagonal of the loop. In other words, there are the sites k and l such that $ikjl$ is a closed loop. In this second case, the effective contribution is

$$- \frac{4t_{ik}t_{kj}t_{jl}t_{li}}{U^3} \left(1 + 20\vec{S}_k \cdot \vec{S}_l \right) \quad (6)$$

The calculation of the dot product $\vec{S}_k \cdot \vec{S}_l$ will be explained later.

The Hamiltonian of formula 2 can also be written in function of the coupling J in the following way :

$$\mathcal{H} = \frac{1}{2} \sum_i \sum_{\vec{\tau}} J_{(i,i+\vec{\tau})} \vec{S}_i \cdot \vec{S}_{i+\vec{\tau}} \quad (7)$$

After having calculated the couplings, the second main part of this projects consists in the calculation of the spin wave dispersion relation.

The next paragraph explains how the spin wave relation dispersion is calculated for a square lattice, with a lattice constant a .

2.2 Calculation of the spin wave dispersion relation for a 2D square lattice

Let's consider a 2D square lattice, with primitive vectors $(a,0)$ and $(0,a)$ and $\{\vec{\tau}\}$ the set of vectors for which we consider the couplings, without taking into account any symmetry. As the lattice is in the antiferromagnetic Néel state, the general idea is to

apply a staggered rotation of the frame, so that in the staggered frame of reference, the classical ground state is ferromagnetic. Then a Holstein-Primakoff transformation is introduced to express the spin operators in function of bosonic operators a and a^\dagger with the aim of expressing the spin wave dispersion relation.

We denote

$$\epsilon_{\vec{\tau}} = \frac{1 + e^{i\vec{Q}\vec{\tau}}}{2} \quad \text{and} \quad \bar{\epsilon}_{\vec{\tau}} = \frac{1 - e^{i\vec{Q}\vec{\tau}}}{2} \quad (8)$$

where $Q = (\frac{\pi}{a}, \frac{\pi}{a}, 0)$

The development of the spin product is made to the first order :

$$\vec{S}_i \cdot \vec{S}_{i+\tau} = S^2 \left[(\vec{S}_i \cdot \vec{S}_{i+\tau})^{(0)} + \frac{1}{S} (\vec{S}_i \cdot \vec{S}_{i+\tau})^{(1)} + \mathcal{O}\left(\frac{1}{S^2}\right) \right] \quad (9)$$

In this development, the terms are expressed in function of the bosonic operators :

$$\begin{aligned} (\vec{S}_i \cdot \vec{S}_{i+\tau})^{(0)} &= 2\epsilon_{\vec{\tau}} - 1 \\ (\vec{S}_i \cdot \vec{S}_{i+\tau})^{(1)} &= (1 - 2\epsilon_{\vec{\tau}})(a_i^\dagger a_i + a_{i+\tau}^\dagger a_{i+\tau}) + 2\epsilon_{\vec{\tau}}(a_{i+\tau}^\dagger a_i + a_i^\dagger a_{i+\tau}) - 2\bar{\epsilon}_{\vec{\tau}}(a_i a_{i+\tau} + a_i^\dagger a_{i+\tau}^\dagger) \end{aligned} \quad (10)$$

Then, substituting the operators by the Fourier transform :

$$\begin{aligned} a_i &= \frac{1}{\sqrt{N}} \sum_{\vec{k}} e^{i\vec{k}\vec{R}_i} a_{\vec{k}} \\ a_i^\dagger &= \frac{1}{\sqrt{N}} \sum_{\vec{k}} e^{-i\vec{k}\vec{R}_i} a_{\vec{k}}^\dagger \end{aligned} \quad (11)$$

The second part of equation 10 becomes, after summation over i :

$$\sum_i (\vec{S}_i \cdot \vec{S}_{i+\tau})^{(1)} = \sum_{\vec{k}} A_{\vec{\tau}} a_{\vec{k}}^\dagger a_{\vec{k}} + \frac{1}{2} B_{\vec{\tau}} (a_{\vec{k}}^\dagger a_{-\vec{k}}^\dagger + a_{\vec{k}} a_{-\vec{k}}) \quad (12)$$

where

$$A_{\vec{\tau}} = 2(1 - 2\epsilon_{\vec{\tau}}) + 2\epsilon_{\vec{\tau}} \cos(\vec{k} \cdot \vec{\tau}) \quad \text{and} \quad B_{\vec{\tau}} = -2\bar{\epsilon}_{\vec{\tau}} \cos(\vec{k} \cdot \vec{\tau}) \quad (13)$$

Finally the spin wave dispersion relation is given by :

$$\omega_{\vec{k}} = \sqrt{A_{\vec{k}}^2 - B_{\vec{k}}^2} \quad (14)$$

where

$$A_{\vec{k}} = \frac{1}{2} \sum_{\vec{\tau}} A_{\vec{\tau}} \cdot J_{(i, i+\vec{\tau})} \quad \text{and} \quad B_{\vec{k}} = \frac{1}{2} \sum_{\vec{\tau}} B_{\vec{\tau}} \cdot J_{(i, i+\vec{\tau})} \quad (15)$$

This relation is valid for one square lattice. The lattice structure we are interested in consists of the superposition of two square sublattices (cf. section 3.1).

The formula 7 can be rewritten by separating the different sublattices (A or B) between which the coupling is calculated :

$$\mathcal{H} = \underbrace{\sum_{\{i,i+\vec{\tau}\} \in A} J_{(i,i+\vec{\tau})} \vec{S}_i \vec{S}_{i+\vec{\tau}}}_{\Rightarrow \omega_{\vec{k}}^{(A)} a_{\vec{k}}^\dagger a_{\vec{k}}} + \underbrace{\sum_{\{i,i+\vec{\tau}\} \in A \text{ and } B} J_{(i,i+\vec{\tau})} \vec{S}_i \vec{S}_{i+\vec{\tau}}}_{\Rightarrow \text{ignore}} + \underbrace{\sum_{\{i,i+\vec{\tau}\} \in B} J_{(i,i+\vec{\tau})} \vec{S}_i \vec{S}_{i+\vec{\tau}}}_{\Rightarrow \omega_{\vec{k}}^{(B)} b_{\vec{k}}^\dagger b_{\vec{k}}}$$

(16)

The approximation is made that we can neglect the term of interaction between the two sublattices to calculate the spinwave. The derivation of the interaction term would be mathematically too complicated, therefore we assume that we can ignore the interaction term of formula 16.

3 Crystal structure

3.1 Plane structure

The compound we are considering is $\text{Sr}_2\text{Cu}_3\text{O}_4\text{Cl}_2$. Its plane structure is illustrated in figure 1

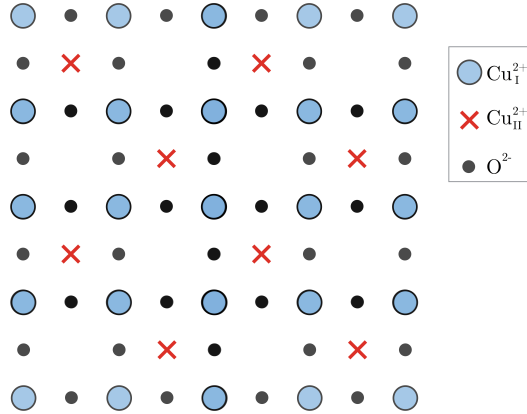


Figure 1: Plane structure of $\text{Sr}_2\text{Cu}_3\text{O}_4\text{Cl}_2$.

In the crystal of $\text{Sr}_2\text{Cu}_3\text{O}_4\text{Cl}_2$, the distance between two atoms of Cu_I^{2+} is equal to 3.859\AA . The atoms of oxygen will not be considered in our one band Hubbard model.

3.2 3D Structure

The space structure of $\text{Sr}_2\text{Cu}_3\text{O}_4\text{Cl}_2$ consists of superposed planes composed of Cu_I^{2+} , Cu_{II}^{2+} and O^{2-} . Between two of these planes, there are two intermediary planes, one with Cl^- atoms and the other with Sr^{2+} atoms. In figure 2, we observe that the planes of Cu_I^{2+} , Cu_{II}^{2+} and O^{2-} are not strictly superposed but there is an additional translation

between the planes. Still in figure 2, we see that the two sublattices of Cu_I^{2+} and Cu_{II}^{2+} are represented with the spins, aligned according to the antiferromagnetic Neel state.

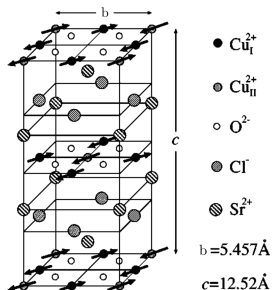


Figure 2: Reciprocal lattice of the plane structure of $\text{Sr}_2\text{Cu}_3\text{O}_4\text{Cl}_2$.

4 Reciprocal space

From now, we assume that the size between two atoms of Cu_I^{2+} is equal to 1. The reciprocal lattice of the plane structure of the compound is given in figure 3.

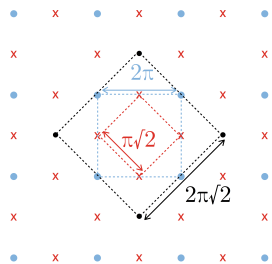


Figure 3: Reciprocal lattice of the plane structure of $\text{Sr}_2\text{Cu}_3\text{O}_4\text{Cl}_2$.

Each sublattice in the real space (Cu_I^{2+} , Cu_{II}^{2+} and O^{2-}) is associated to a square lattice in the reciprocal space, whose periodicity is inversely proportionnal to the size of unit cell in real space.

5 Coupling between two sites

5.1 Description of the algorithm

The hoppings that are considered to be possible and the associated hopping energy is shown in figure 4.

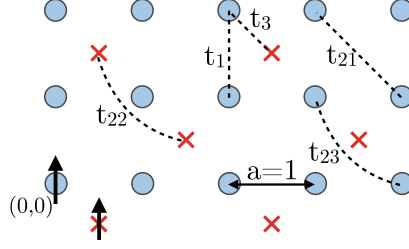


Figure 4: The possible hoppings on the lattice and the associated hopping energy.

The hopping energy t_1 is associated to any hopping of length 1 (between two neighbour Cu_I^{2+}), since all of them are equivalent regarding the symmetry of the lattice. For the same reason, the hopping energy between an Cu_{II}^{2+} atom and any of the nearest neighbour Cu_I^{2+} is t_3 .

However, for the hopping of length $\sqrt{2}$, there are three cases, and we cannot consider that the associated energy are the same. Therefore we have the energy t_{21} , t_{22} and t_{23} . The main part of the algorithm to compute the coupling between two given points is to define all the possible paths of a given length n that goes from one site A to another site B . The main steps of the algorithm are the following :

- Define a function that takes as argument the coordinates of one point and that returns all the possible hoppings from this point. As each of the lattice is not equivalent, the aim of this function is to never reach an empty site.
- Consider all the possible combinations of length n that start from A . All the possible paths that do not end at B are then removed. On the remaining paths from A to B , we have to ensure that one site is not crossed two times. If it is the case, the possibility is also removed.

In formulas 5 and 6 there is the product of spin $\vec{S}_k \cdot \vec{S}_l$. To calculate this term, the assumption is made that each sublattice (Cu_I^{2+} and Cu_{II}^{2+}) is in the antiferromagnetic Neel state and one spin on each of them is arbitrarily defined (See figure 4 for the position of origin and the determination of the up spin on each of the sublattices.) The coupling is then calculated as described in equations 3 to 6.

5.2 Results

5.2.1 Analytical expression for couplings

Let us begin with couplings between two sites separated by a distance 1.

(0,0)	(1,0)	$-\frac{64t_1^4}{U^3} - \frac{8t_3^2t_1^2}{U^3} - \frac{48t_{21}t_{23}t_1^2}{U^3} - \frac{16t_3^2t_{21}t_1}{U^3} - \frac{48t_3^2t_{22}t_1}{U^3} - \frac{16t_3^2t_{23}t_1}{U^3} + \frac{4t_3^4}{U^3} + \frac{4t_1^2}{U}$
(0,0)	(0,-1)	
(1,1)	(1,2)	
(1,1)	(0,1)	
(0,0)	(-1,0)	
(0,0)	(0,1)	
(1,1)	(2,1)	
(1,1)	(1,0)	

Table 1: Coupling between two sites separated by a distance 1.

(1,0)	($\frac{1}{2}, -\frac{1}{2}$)	$-\frac{16t_3^4}{U^3} + \frac{4t_{22}^2t_3^2}{U^3} + \frac{4t_{23}^2t_3^2}{U^3} + \frac{32t_{21}t_{22}t_3^2}{U^3} + \frac{16t_1t_{23}t_3^2}{U^3} + \frac{8t_{22}t_{23}t_3^2}{U^3} - \frac{64t_1^2t_3^2}{U^3} - \frac{16t_1t_{21}t_3^2}{U^3} - \frac{64t_1t_{22}t_3^2}{U^3} + \frac{4t_3^2}{U}$
(0,1)	($\frac{1}{2}, \frac{3}{2}$)	
(0,0)	($-\frac{1}{2}, \frac{1}{2}$)	
(1,1)	($\frac{3}{2}, \frac{1}{2}$)	
(0,0)	($\frac{1}{2}, -\frac{1}{2}$)	$-\frac{16t_3^4}{U^3} + \frac{4t_{22}^2t_3^2}{U^3} + \frac{4t_{23}^2t_3^2}{U^3} + \frac{16t_1t_{22}t_3^2}{U^3} + \frac{16t_1t_{23}t_3^2}{U^3} - \frac{64t_1^2t_3^2}{U^3} - \frac{16t_1t_{21}t_3^2}{U^3} - \frac{48t_{21}t_{22}t_3^2}{U^3} - \frac{32t_{22}t_{23}t_3^2}{U^3} + \frac{4t_3^2}{U}$
(1,1)	($\frac{1}{2}, \frac{3}{2}$)	
(1,0)	($\frac{3}{2}, \frac{1}{2}$)	
(0,1)	($-\frac{1}{2}, \frac{1}{2}$)	

Table 2: Coupling between two sites separated by a distance $1/\sqrt{2}$

(0,0)	(1,1)	$-\frac{16t_1^4}{U^3} + \frac{32t_{21}^2t_1^2}{U^3} - \frac{32t_{21}t_{23}t_1^2}{U^3} - \frac{16t_3^2t_{21}t_1}{U^3} + \frac{32t_{21}^2t_{23}^2}{U^3} - \frac{16t_{21}^4}{U^3} - \frac{48t_3^2t_{21}t_{22}}{U^3} + \frac{4t_{21}^2}{U}$
(1,0)	(0,1)	
(0,0)	(1, -1)	$-\frac{16t_1^4}{U^3} + \frac{32t_3^2t_1^2}{U^3} + \frac{32t_{23}^2t_1^2}{U^3} - \frac{32t_{21}t_{23}t_1^2}{U^3} - \frac{96t_3^2t_{23}t_1}{U^3} + \frac{4t_3^4}{U^3} + \frac{32t_{21}^2t_{23}^2}{U^3} - \frac{16t_{23}^4}{U^3} - \frac{48t_3^2t_{22}t_{23}}{U^3} + \frac{4t_{23}^2}{U}$
(0,0)	(-1,1)	
(2,0)	(0, -1)	
(2,0)	(2,1)	
(1/2, -1/2)	(3/2, -3/2)	$\frac{4t_3^4}{U^3} + \frac{32t_{21}t_{22}t_3^2}{U^3} + \frac{32t_{22}t_{23}t_3^2}{U^3} - \frac{96t_1t_{22}t_3^2}{U^3} - \frac{64t_{22}^4}{U^3} + \frac{4t_{22}^2}{U}$
	(3/2, 1/2)	

Table 3: Coupling between two sites separated by a distance $\sqrt{2}$.

(0,0)	(0,±2)	$\frac{4t_1^4}{U^3} + \frac{32t_{21}t_{23}t_1^2}{U^3} - \frac{16t_{21}^2t_{23}^2}{U^3}$
(0,0)	(±2,0)	
(0,1)	(0,1) + (0, ± 2)	
(0,1)	(0,1) + (±2,0)	
($\frac{1}{2}, -\frac{1}{2}$)	($\frac{1}{2}, -\frac{1}{2}$) + (0, ±2)	$-\frac{16t_{22}^4}{U^3}$
($\frac{1}{2}, -\frac{1}{2}$)	($\frac{1}{2}, -\frac{1}{2}$) + (±2, 0)	
($\frac{1}{2}, \frac{3}{2}$)	($\frac{1}{2}, \frac{3}{2}$) + (0, ±2)	
($\frac{1}{2}, \frac{3}{2}$)	($\frac{1}{2}, \frac{3}{2}$) + (±2, 0)	
(0,0)	(±2, ±4)	$\frac{4t_{21}^2t_1^2}{U^3} + \frac{4t_{23}^2t_1^2}{U^3} + \frac{16t_{21}t_{23}t_1^2}{U^3}$
(0,0)	(±4, ±2)	

Table 4: Couplings extended to further neighbour.

Finally, for any two sites separated by $2\sqrt{2}$, the total coupling is equal to the three sites coupling :

(0,0)	±(2,2)	$\frac{4t_{21}^4}{U^3}$
(1,0)	(3, - 2); (-1,2)	
(0,0)	±(-2,2)	$\frac{4t_{23}^4}{U^3}$
(1,0)	(3,2); (-1, - 2)	
($\frac{1}{2}, -\frac{1}{2}$)	($\frac{1}{2}, -\frac{1}{2}$) + (±2, ± 2)	$\frac{4t_{22}^4}{U^3}$

5.2.2 Plots in function of t_3

Until now, we have distinguished t_{21} , t_{22} and t_{23} , we will assume that the numerical value of the hopping is the same. The main reason is that the goal of this section is to highlight the influence of the hopping t_3 , and not to determine the consequence of different t_2 .

The numerical values for t_1 , t_{2i} and U are taken from the article [2] for the BSYCO compound.

	[meV]
t_1	470
$t_{2i} ; i = 1,2,3$	-205
U	3500

In the following figures, the value of the coupling is calculated in function of t_3 .

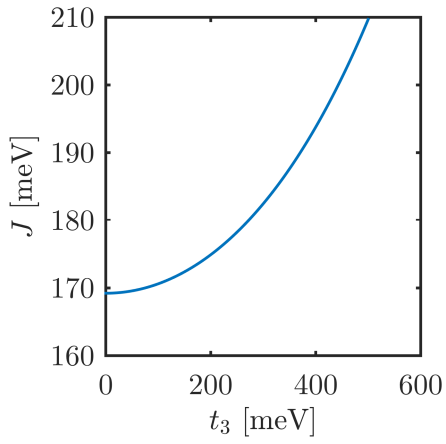


Figure 5: Coupling between (0,0) and (1,0)

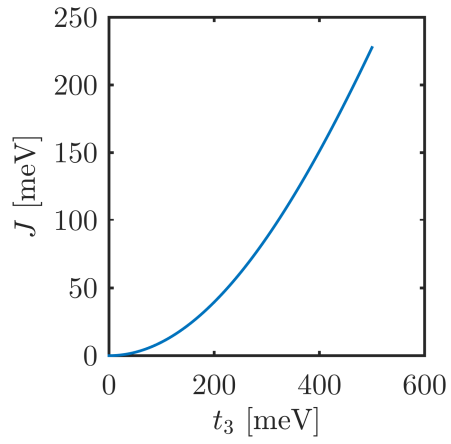


Figure 6: Coupling between (0,1) and (1/2,3/2)

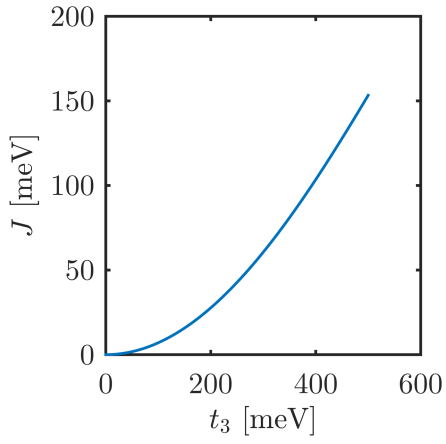


Figure 7: Coupling between (1,1) and (1/2,3/2).

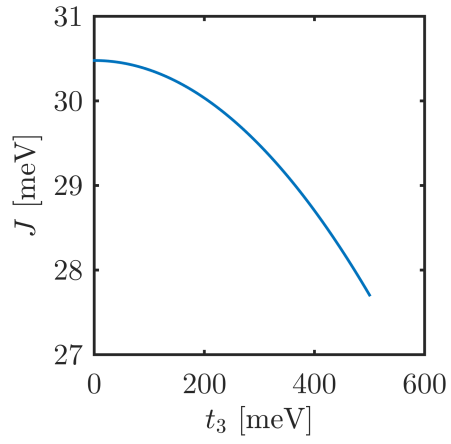


Figure 8: Coupling between (0,0) and (1,1)

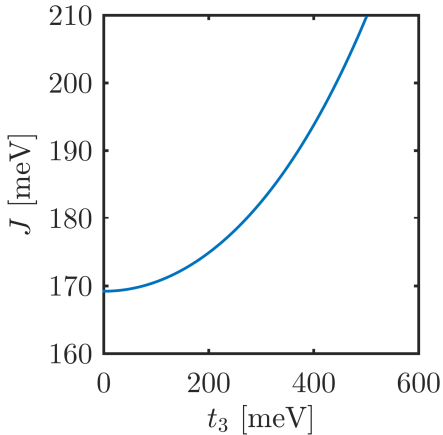


Figure 9: Coupling between (2,0) and (2,1)

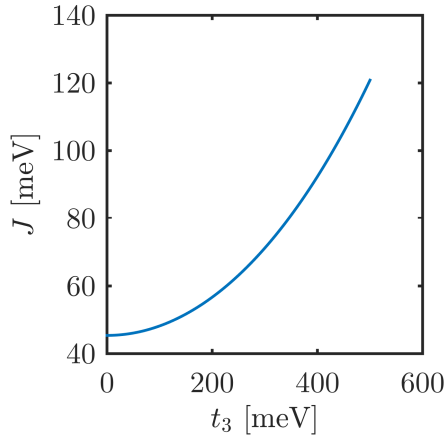


Figure 10: Coupling between (1/2, -1/2) and (3/2, 1/2)

All the couplings increase with t_3 except $J_{(0,0),(1,1)}$ which decreases with t_3 . Indeed, in this case the evolution is mainly determined by the term $\frac{-48t_3^2 t_{21} t_{22}}{U^3}$. Generally, the dominant term is due to the direct coupling ($\propto 1/U$) if the two sites are directly connected, and otherwise to the indirect or quartic coupling.

6 Spin wave relation dispersion

6.0.2.1 definition of parameters for the simulation

- Cu_I^{2+} **Lattice** :

The vectors $\vec{\tau}$ that are considered to calculate the spin wave are (on the quarter plane): $\{(0,1), (0,2), (1,2), (1,1), (2,2), (2,1)\}$. By applying successive $\pi/2$ rotations, we finally obtain a total of 24 $\vec{\tau}$ considered in the sum.

The vector \vec{Q} is equal to (π, π) .

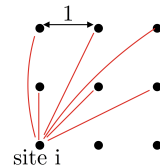


Figure 11: The vectors $\vec{\tau}$, only represented on the quarter of the plane

- Cu_{II}^{2+} **Lattice** : the reasoning is exactly the same, and the set of $\vec{\tau}$ as well as \vec{Q} are obtained by making a rotation of $-\pi/4$ and a rescaling of a factor $\sqrt{(2)}$ for $\vec{\tau}$ and $1/\sqrt{(2)}$ for \vec{Q} . Therefore, $Q = (\pi, 0)$.

The lattice that we have considered until now can be decomposed in two square sublattices, one composed of Cu_I^{2+} (the reference to this lattice) and the other Cu_{II}^{2+} . Note that, from now on, we take $t_3 = 200$ meV.

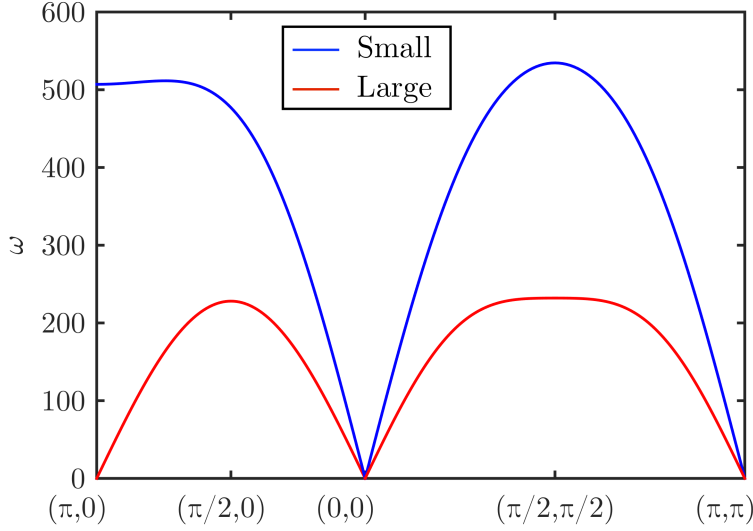


Figure 12: Superposition of the dispersion relation for both Cu_I^{2+} and Cu_{II}^{2+} lattices

On figures 12, we can see that the points in the k -space $(0,0)$ and $(\pi,0)$ associated to the large lattice are equivalent in the sense that $\omega_{\vec{k}}$ goes to 0 (Goldstone mode) as well as $(0,0)$ and (π,π) associated to the small one are equivalent. This equivalence is due to the periodicity of the spin in the antiferromagnetic Neel state : indeed if we consider the small lattice, we have up spin at the origin $(0,0)$ and at $(1,1)$. The lattice that consists on up spins is a square lattice with lattice constant $\sqrt{2}$ and rotated of $\pi/4$ with respect to the whole lattice. This periodicity leads to a periodicity of $2\pi/\sqrt{2} = \pi\sqrt{2}$ in the momentum space, still rotated by $\pi/4$. This is why the points $(0,0)$ and (π,π) are equivalent. By analogy, this is also the reason why $(0,0)$ and $(\pi,0)$ are equivalent when considering the Cu_{II}^{2+} lattice.

A small difference in the value of ω_k is observed, depending on which point of the lattice is considered as origin for the Cu_I^{2+} lattice . The figure 13 illustrates this difference. Furthermore, comparatively to the figure 12, the zone boundary is added.

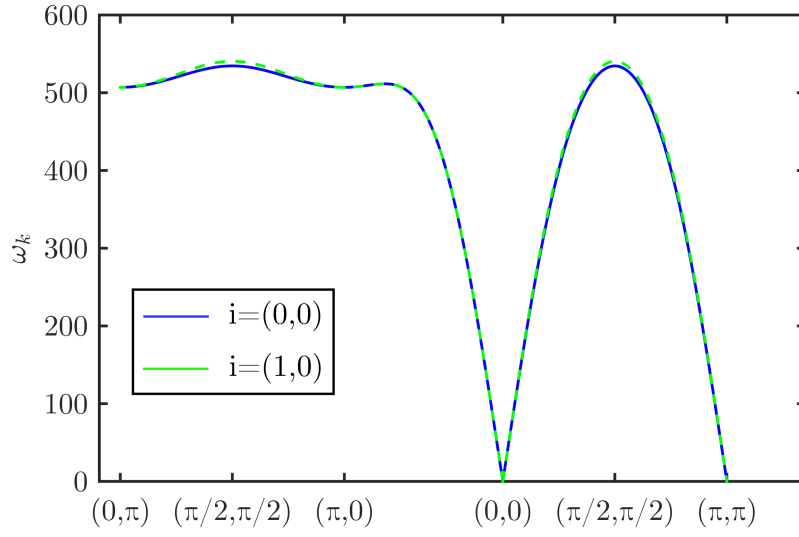


Figure 13: Comparison of ω_k , depending on the origin (site i) that is considered

This difference corresponds to the fact that the actual unit cell of the whole structure is larger than the unit cell of the small sublattice. Hence we observe an additional band. Finally, the zone boundary on the large lattice with the zone boundary is shown in figure 14

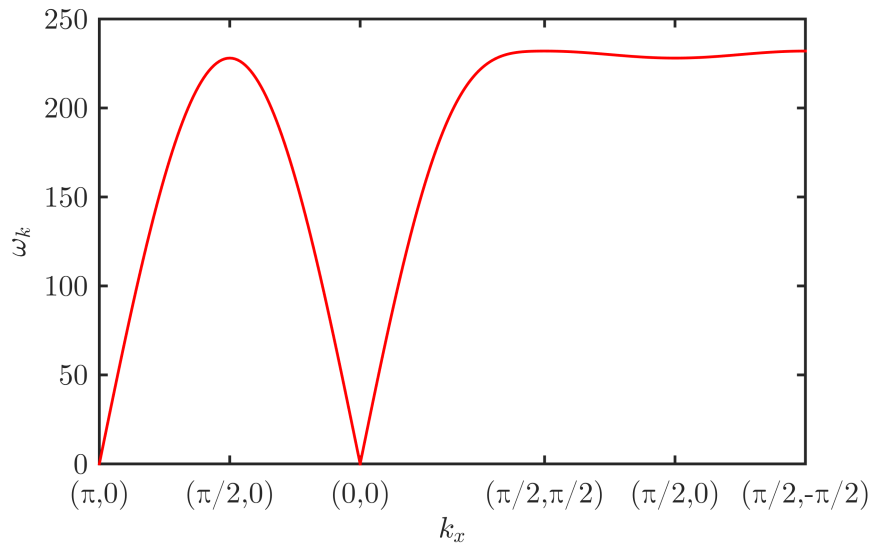


Figure 14: Zone Boundary on the large lattice

We can see that the fluctuations along the zone boundary are less important on the large lattice than on the small one.

7 Conclusion

During this project, we have determined some magnetic properties in a compound that have the same structure of the $\text{Sr}_2\text{Cu}_3\text{O}_4\text{Cl}_2$ compound. In particular, we have provided analytical expressions for couplings and we have shown the role played by t_3 .

We have calculated the spin wave dispersion at $t_3 = 200$ meV for each of the sublattice that forms the crystal. In order to do this, there were need to extend the possible hoppings to the third nearest neighbour. We have seen that the fluctuations along the zone boundary are more important on the small square lattice, and the maximum of ω_k is about 2.3 times larger for the small sublattice than for the large one (still with $t_3 = 200$ meV).

In a future work, a major improvement would be to take into account the interactions terms in the calculation of the spin wave. It would also be interesting to determine more precisely the numerical values of the hopping energy, especially by considering different hoppings energies for the t_2 .

8 References

- [1] B. DALLA PIAZZA, Theories of Experimentally Observed Excitation Spectra of Square Lattice Antiferromagnets, 2014, Lausanne
- [2] B. DALLA PIAZZA & al. , Unified one-band Hubbard model for magnetic and electronic spectra of the parent compounds of cuprate superconductors, Physical Review B 85, 100508(R), 2012
- [3] Y. KIM & al., Neutron Scattering Study of $\text{Sr}_2\text{Cu}_3\text{O}_4\text{Cl}_2$, Physical review B, VOLUME 64, 024435, 2001.